



Cretaceous and Paleogene granitoid suites of the Sikhote-Alin area (Far East Russia): Geochemistry and tectonic implications



Andrei V. Grebennikov^{a,b,*}, Alexander I. Khanchuk^a, Valeriy G. Gonevchuk^a, Sergey V. Kovalenko^c

^a Far East Geological Institute, Far Eastern Branch of the Russian Academy of Sciences, 159, Prospekt 100-letiya Vladivostok, Vladivostok 690022, Russian Federation

^b Far Eastern Federal University, 8, Sukhanova St., Vladivostok, 690950, Russian Federation

^c Primorgeology, Okeansky Prospekt 29/31, Vladivostok 690091, Russian Federation

ARTICLE INFO

Article history:

Received 5 July 2015

Accepted 21 December 2015

Available online 5 January 2016

Keywords:

A- S-, and I-type granites

Petrochemical classification

Tectonic setting, Sikhote-Alin, Russian Far East

ABSTRACT

The Mesozoic and Cenozoic geological history of NE Asia comprises alternating episodes of subduction or transform strike-slip movement of the oceanic plate along the continental margin of Eurasia. This sequence resulted in the regular generation of granitoid suites that are characterized by different ages, compositions, and tectonic settings. The Hauterivian–Aptian orogenic stage of the Sikhote-Alin, associated with the strike-slip displacement of the early Paleozoic continental blocks, the successive deformation of the Jurassic and Early Cretaceous terranes, and the injection of the earliest S-type granitoids. During late Albion, the area underwent syn-strike-slip compression caused by collision with the Aptian island arc and resulted in the injection of voluminous magmas of calc-alkaline magnesian (S- and I-type) and alkali-calcic ferroan (A-type) granitoids into syn-faulting compressional and extensional basins, respectively. Northwestward to westward movement of the Izanagi Plate resulted in the initiation of frontal subduction of the Paleo-Pacific Plate during the Cenomanian–Maastrichtian. In turn, this resulted in the generation of plateau-forming ignimbrites and their intrusive analogs formed from metaluminous I-type felsic magmas. Paleocene–Eocene magmatism in the Sikhote-Alin area commenced after the termination of subduction in a rifting regime related to strike-slip movement of the oceanic plate relative to the continent. The break-off of the subducted plate and the injection of oceanic asthenospheric material into the subcontinental lithosphere resulted in the eruption of lamproites and fayalite rhyolites, and coeval intrusions of gabbro and alkali feldspar granites (A-type). The A-type granitic-rocks and coeval gabbro–monzonites are considered to be reliable indicators of the transform continental margin geodynamic settings.

© 2016 Elsevier B.V. All rights reserved.

1. Introduction

The continental area bordering the NW Pacific Ocean has a heterogeneous structure that is a result of the large-scale horizontal displacement of lithospheric plates at continent–ocean boundaries (e.g., Khanchuk (2006), and references therein). The Mesozoic and Cenozoic history of the Pacific margin reflects alternating subduction and transform strike-slip movement of the oceanic plate relative to the continental margin (Khanchuk and Ivanov, 1999; Khanchuk and Kemkin, 2003). Thus, the Sikhote-Alin–North Sakhalin accretionary orogenic belt (herein referred to as the Sikhote-Alin) is a favorable natural laboratory for research on the evolving granitoid magmatism resulting from regional tectonic changes.

Recent data on the tectonics, geodynamics, seismicity, magmatism, and minerals of the Sikhote-Alin (Faure and Natal'in, 1992; Golozubov, 2006; Jahn et al., 2015; Kemkin, 2012; Khanchuk, 2006;

Natal'in, 1993; Nokleberg et al., 2000; Parfenov et al., 2010; Şengör and Natal'in, 1996; Utkin, 2013) have helped to identify the main features of the Mesozoic and Cenozoic tectonic history of the Russian Far East continental margin. The tectonic evolution of this area was dominated by strike-slip movement between the continental and oceanic lithospheric plates, involving large plate margin displacements of hundreds or thousands of kilometers, and the initiation of the proto-Central Sikhote-Alin Fault, which is proposed to have controlled the formation of pull-apart basins and the development of numerous magmatic complexes, including A-type granites. The compositions of these granites reflect the complex interplay between intracrustal melts, mantle-derived magmas, and sediments. Coeval intrusions that host gabbros to monzonites and trachybasalts to trachyandesites give evidence of A-type rocks related to mantle-derived magmas. Extension zones developed in the course of transformation of the convergent boundary subduction into a strike-slip-dominated tectonic regime, and this change, combined with the discrete permeability of continental lithosphere, allowed mantle-derived melts to ascend (Khanchuk et al., 1997).

A-type magmatic rocks in a strict sense have not been previously identified in the Sikhote-Alin area (we, however, do not ignore sporadic

* Corresponding author at: Far East Geological Institute, Far Eastern Branch of the Russian Academy of Sciences, 159, Prospekt 100-letiya Vladivostok, Vladivostok 690022, Russian Federation. Tel.: +7 9147050037.

E-mail address: greandr@hotmail.com (A.V. Grebennikov).

identifications of this type described in earlier publications, by Jahn et al. (2015), for example), mainly because existing geochemical discrimination diagrams (e.g., Eby (1992); Pearce et al. (1984) and Whalen et al. (1987)) do not differentiate between peraluminous silicic magmas derived from contaminated mantle A-type melts and crustal I- and S-type melts.

This paper summarizes our current understanding of the geodynamic development of the Sikhote-Alin area since the Early Cretaceous, based on existing data related to the regional stratigraphy, metamorphism and tectonics. After considering the occurrence and compositional characteristics of granitoid magmatism (and particularly A-type granites) in the context of their formation during certain geodynamic stages, we propose a new paleogeodynamic model for the Sikhote-Alin area.

2. Geological background

2.1. Geodynamic evolution of the Sikhote-Alin, since the Early Cretaceous

The Sikhote-Alin area represents a collage of terranes of different origins and ages, accreted during the Mesozoic to Cenozoic (e.g., Khanchuk (2006); Khanchuk and Ivanov (1999); Khanchuk et al. (1997); Natal'in (1993); Nokleberg et al. (2000), (2003) and Parfenov et al. (2010)). In the Jurassic, increased subduction of oceanic lithosphere resulted in the accretion of remote continental blocks and island arcs to the margin of the Siberian Craton (e.g., Kemkin (2008) and Natal'in (1993)). During this process, large accreted blocks fragmented into terranes and formed a late Albian–early Cenomanian orogenic belt (Khanchuk, 2001). The accretion of terranes during the Jurassic–Early Cretaceous caused changes in the geodynamic setting along the newly formed continental margin. From the Early Cretaceous to the Eocene, the geodynamic setting changed from Pacific Plate-type transform strike-slip movement (in the late Albian) to an active Andean-type margin (Cenomanian–Maastrichtian), before changing back to transform-type tectonism (Paleocene–Eocene; Khanchuk and Ivanov, 1999). At each of these stages, the craton margins and terranes were stitched together by granitoid batholiths and volcanic–plutonic belts. During the late Cenozoic, rifting and extension formed the depressions of the seas of Japan and Okhotsk, accretion at the Asian continental margin ceased, and the setting changed to a destructive regime (Khanchuk, 2006, and references therein).

In this paper, we use the term Sikhote-Alin to refer to an Early Cretaceous orogenic belt on the Russian Far East continental margin that is unconformably overlain by undeformed Upper Cretaceous and Cenozoic volcanic and sedimentary units. The belt is up to 600 km wide and extends northeastward for ~1500 km from the southern boundary of Primorye to the Amur River mouth and northern margin of Sakhalin Island. The belt is bounded to the west by the early Paleozoic Bureya–Khanka orogenic belt and to the north by the Early Cretaceous Mongol–Okhotsky belt. The Sikhote-Alin contains numerous terranes, including fragments of Jurassic and Early Cretaceous accretionary prisms, and Early Cretaceous terranes formed in an island arc system and in a syn-faulting turbidite basin (Fig. 1). The tectono-stratigraphic sequence in this area suggests that the terrigenous matrix of the accretionary prism formed on top of oceanic crust after the Callovian, in a tectonic setting analogous to those found in present-day deep-sea trenches (Khanchuk, 2006).

During the Mesozoic and Cenozoic, the Sikhote-Alin area was the site of alternating stages of voluminous orogenic and post-orogenic magmatism in the form of numerous intrusive complexes that have common petrographic, geochemical, and geochronological features.

2.2. Hauterivian–Aptian igneous episode (130–120 Ma)

The injection of the earliest (Khungari) granitoids within the Sikhote-Alin was associated with the displacement of the early

Paleozoic continental lithosphere, the successive deformation of the Jurassic and Early Cretaceous terranes, and the generation of a metamorphosed granite layer (Khanchuk et al., 2013).

2.2.1. Khungari granitoids

The Khungari granitoids crop out in several batholith-like (>100 km²) Hauterivian–Aptian massifs that are generally located within the area around the Central Sikhote-Alin Fault (48°00′–50°30′N), and in the Bikinsky zone (46°30′–47°30′N) some 100 km west of the central suture. Small intrusive bodies occur in the early Paleozoic Khanka orogenic belt (44°50′–45°10′N; e.g., Izokh et al. (1967); Simanenkov et al. (1997); Fig. 2a).

The granitoids intrude the Jurassic sediments and Late Jurassic E–W-striking pyroxenite, gabbroid, and gabbro–diorite dikes, and can be divided into two types: the dominant first type consists of biotite and two-mica cordierite-bearing diorites, quartz–diorites, and melagranites; the second type consists of fine-grained biotite granite and leucogranite. The granitoids have a similar mineral composition. The main felsic minerals are mainly quartz with lesser albite and microcline (Kruk et al., 2014). The margins of these intrusions are enriched in red–brown biotite (up to 15%–20% modal abundance), whereas the cores are enriched in aluminiferous minerals such as muscovite (10%) and cordierite (up to 2%). No amphibole is present, even in the least silicic varieties of these granitoids. The major minerals are accompanied by accessory ilmenite, zircon, monazite, tourmaline, apatite, garnet, and very rare magnetite (Izokh et al., 1967; Martinyuk et al., 1990).

The geochemistry of the Khungari granitoids (Gvozdev, 2010; Izokh et al., 1967; Kruk et al., 2014; Simanenkov et al., 1997) indicates that they are peraluminous and are S-type granites according to the definition of Chappell and White (1974). These granitoids have moderate alkalinity, are predominantly potassic, and contain moderate concentrations of iron. In the classification diagrams of Frost et al. (2001; Fig. 3a–b), they are considered calc-alkalic, alkali-calcic, ferroan, and magnesian. According to the graph of Liégeois and Black (1987; Fig. 3d), they are calc-alkaline rocks. The majority of these granitoids also plot in the volcanic arc granite (VAG) field on the tectonic discrimination diagram of Pearce et al. (1984) and as orogenic granitoids on classification diagrams based on Zr, Nb, Ce, and Y (Whalen et al., 1987; Fig. 3e) and based on the molecular quantities of rock-forming oxides (Grebennikov, 2014; Fig. 3f).

Previous research indicates that the Khungari granitoids intruded Berriasian–Hauterivian sediments that show evidence of contact metamorphism, and are overlain by Barremian–Aptian units, indicating that the granitic rocks formed during the Valanginian–Hauterivian (Izokh et al., 1967; Martinyuk et al., 1990; Nazarenko and Bazhanov, 1987). Recent Rb–Sr isotopic dating yields ages of 123.7 ± 0.8 Ma ($^{87}\text{Sr}/^{86}\text{Sr}_i = 0.70909$) to 125.6 ± 0.9 Ma ($^{87}\text{Sr}/^{86}\text{Sr}_i = 0.70949$; Khetchikov et al., 1997, 1998), and U–Pb – 131.4 ± 2.0 Ma (Jahn et al., 2015) that are consistent with the geological relationships described above. These ages are comparable to U–Pb zircon ages from the Hamahe batholith (124 Ma) and granites in the Raohe Complex (128 Ma) of northeastern China (Cheng et al., 2006; Zhou et al., 2014). The Khungari granitoids formed from magmas generated from a source with a major component of metasediments from the Samarka terrane ($\epsilon_{\text{Nd}} = -3.7$ to -4.1 ; Kruk et al., 2014) and that also contained fragments of late Paleozoic and early Mesozoic oceanic crustal material (e.g., basalt, chert, and limestone).

The largest occurrence of tungsten mineralization associated with the Khungari granitoids is the scheelite–quartz ore of the Lermontovskoe deposit (~120 Ma from K–Ar and Rb–Sr dating; Gvozdev, 2010).

2.3. Late Albian igneous episode (110–98 Ma)

During the late stages of orogeny, the Sikhote-Alin area underwent syn-strike-slip compression caused by collision with the Kema island

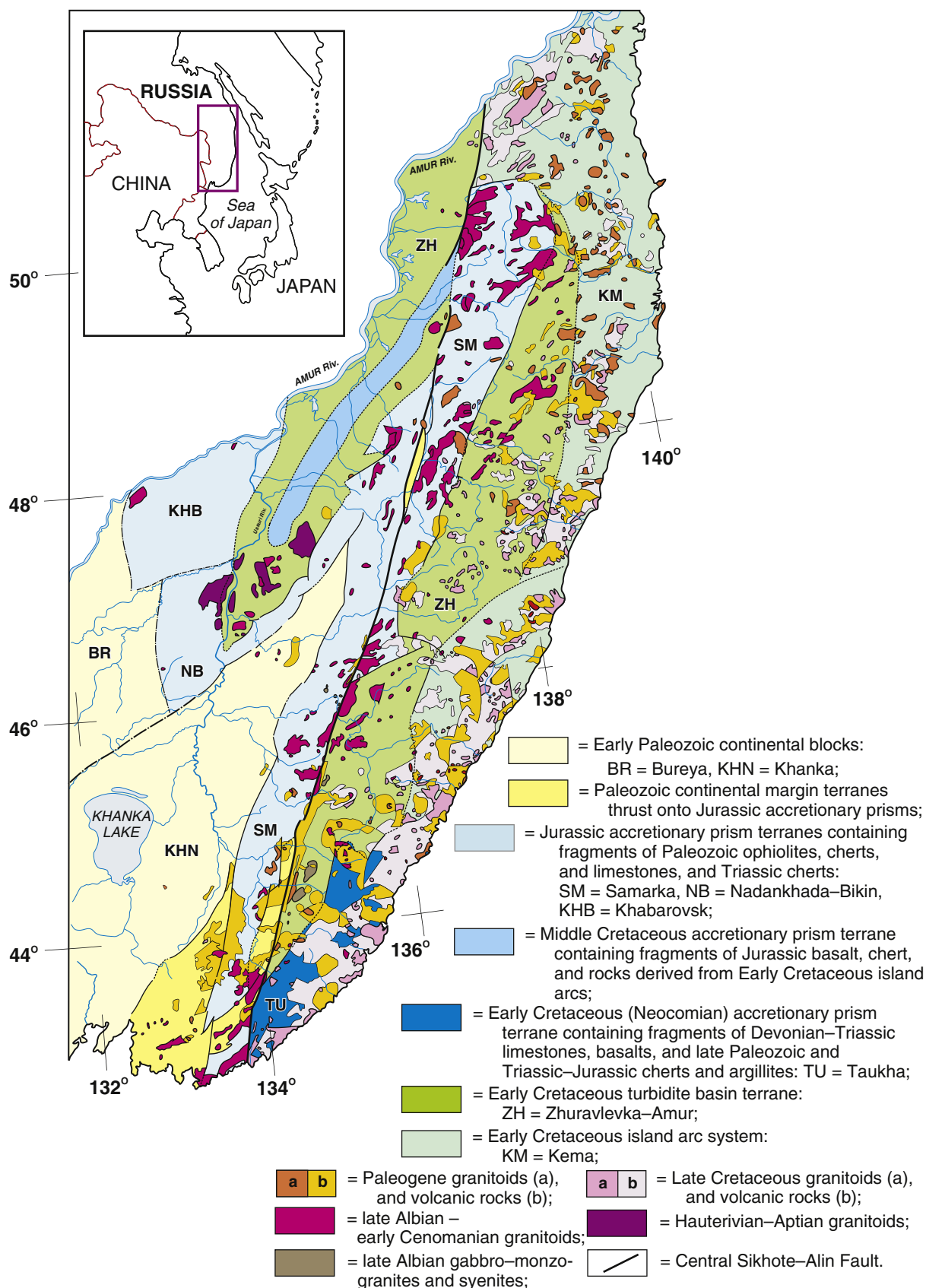


Fig. 1. Geologic map of the Sikhote-Alin (Primorye) area of Far East Russia (modified after Krasnyi et al. (1996)).

arc (e.g., Golozubov (2006); Khanchuk (2001) and Khanchuk et al. (1996)). This resulted in the injection of voluminous granitoid magmas into syn-faulting extensional or compressional basins.

The Albian granitoids crop out within a zone that borders the Central Sikhote-Alin Fault. These rocks form several large massifs that have no volcanic analogs, although the NW part of the Sikhote-Alin area

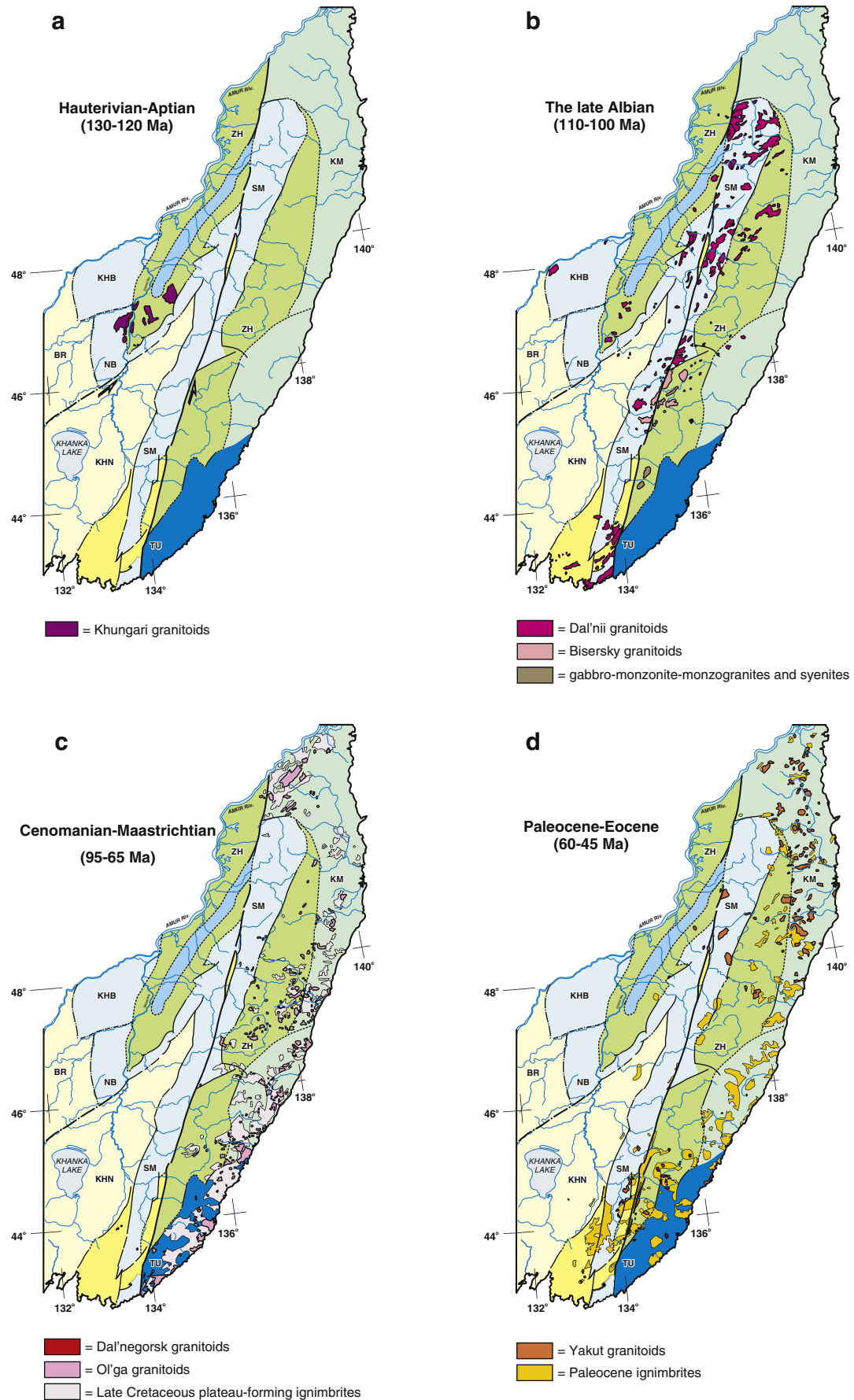


Fig. 2. (a–d) A geological sketch of the Sikhote-Alin area of Far East Russia. Terrane names are the same as in Fig. 1.

contains the analogous Myao–Chansky magmatic series (Gonevchuk, 2002; Izokh et al., 1967; Rub et al., 1986). These intrusive massifs, which are generally referred to as the Tatiba series (Nazarenko and Bazhanov, 1987), consist of coeval granitoids that were emplaced in different tectonic settings and have different chemical compositions. Two paragenetically associated granitoid types are identified within this series: the Dal'nii type and the Biser type (Ivanov et al., 1980; Izokh et al., 1967; Levashev, 1991; Simanenko et al., 1997). These massifs commonly occur in the same area and form magmatogene domes.

Recent research has identified three phases of granitoid formation within this series. The initial phase is characterized by the intrusion of diorites, quartz-diorites, and monzogranites; the second phase by the intrusion of quartz-diorite and biotite–hornblende and biotite granite; and the third phase by the intrusion of porphyritic granite and leucocratic granite. The massifs in the study area have highly variable proportions of these three phases. Some massifs (Dal'nii type) are dominated by first-phase rocks, whereas others (Biser type) are dominated by second- and third-phase medium- to coarse-grained biotite and leucocratic granites.

2.3.1. Dal'nii granitoids

The majority of the Dal'nii granitoids crop out between the latitudes of 45°30'N and 46°45'N, as well as to the south (42°40'N–43°00'N; Uspensky massifs) and north (47°50'N–48°50'N; Sandinsky massifs) of this interval (Fig. 2b). These granitoids intruded terrigenous and volcanogenic sediments of the Samarka terrane within a Jurassic accretionary prism, and partly a sequence of arkosic sandstones and siltstones (~15 km thick) of an Early Cretaceous turbidite basin terrane (Khanchuk, 2006, and references therein).

The intrusions are composed mostly of medium-grained biotite and biotite–hornblende quartz-diorites and melanogranites. Diorites, quartz-diorites, and monzodiorites have been recognized as the earliest intrusive phase. These early intrusions are rich in amphibole and contain sparse pyroxene, whereas the latest intrusions include dikes and small bodies of biotite granite–porphyry and leucocratic granites. The rocks of the intermediate and most voluminous intrusive phase are characterized by the predominance of plagioclase over alkali feldspar, elevated contents of dark-colored minerals, and light brown biotite. Accessory minerals include apatite, zircon, and ilmenite, and the rocks also contain sparse magnetite, scheelite, sphene, rutile, monazite, and allanite (Kruk et al., 2014).

These rocks contain 65–71 wt.% SiO₂ and in general are moderately alkaline (Na₂O + K₂O = 4.2 to 10.05 wt.%), with higher potassium than sodium contents, peraluminous, and rarely metaluminous, according to the Shand A/CNK index (Shand, 1943; Fig. 3c). The Dal'nii granitoids are classified as calc-alkaline (Liégeois and Black, 1987; Fig. 3d), calcic, magnesian, and ferroan on the diagrams of Frost et al. (2001; Fig. 3a–b) and define a nearly continuous trend from S- to I-type granites in the Chappell and White (1974) classification, with the majority of samples being classified as intermediate between these two types (Fig. 3c). Most of these rocks are classified as volcanic arc and syn-collisional granite on the tectonic discrimination diagram of Pearce et al. (1984). The Zr, Nb, Ce, and Y contents of these granitoids indicate that they are orogenic granitoids or highly differentiated quartz-feldspathic granitoids in the classification diagram of Whalen et al. (1987; Fig. 3e), which suggests that they are not typical A-type granites. The discrimination diagram of Grebennikov (2014; Fig. 3f) gives a similar result. These granitoids are also characterized by slightly negative ε_{Nd} values (−0.7 to −3.8; Kruk et al., 2014; Moskalenko et al., 2011).

2.3.2. Biser granitoids

The Biser granitoids intruded a sequence of arkosic sandstones and siltstones (~15 km thick) within a syn-tectonic turbidite basin of the Early Cretaceous Zhuravlevka–Amur terrane. They crop out between the latitudes of 46°30'N and 46°45'N (Fig. 2b). Granite-dominated massifs (e.g., Dal'nearminsky and Vodorazdel'nyi) within the collisional

suture show no clear relationship to the orogenic complexes (Levashev et al., 1989). These medium- to coarse-grained biotite and leucogranites contain approximately equal proportions of quartz, plagioclase, and alkali feldspar. Accessory minerals are similar to those in the Dal'nii granitoids, but with much lower contents of apatite and higher contents of allanite and monazite. The granitoids also contain rare topaz, cassiterite, and four varieties of garnet. A characteristic mineral in these granitoids is ilmenite, which is locally replaced by late-stage magnetite (Khanchuk, 2006; Levashev, 1991). These granitoids are more silicic than the Dal'nii granitoids (SiO₂ of 70–77 wt.%) and are alkali-rich (Na₂O + K₂O = 7.5 to 9.1 wt.%; Pezhenina and Uglov, 2008). They are also classified as alkali-calcic, calc-alkaline, ferroan and uniformly A-type in the classification diagrams of Frost et al. (2001) and Grebennikov (2014; Fig. 3).

K–Ar ages for the Tatiba series range from 105 to 85 Ma (Gonevchuk et al., 2011; Zimin et al., 1991). These rocks also yield highly variable Rb–Sr isochron ages, ranging from 128 ± 1.6 Ma (monzonites) to 112 ± 4.0 Ma (plagiogranites) and 98 ± 1.5 Ma (leucogranites; Khetchikov et al., 1997). Massifs of the Dal'nii complex yield weighted mean U–Pb ages of 103.5 ± 0.8 Ma (Alenicheva et al., 2008), 105.9 ± 1.0 Ma and 108.8 ± 0.8 Ma (Jahn et al., 2015), and 103.3 ± 2.4 Ma (Khanchuk et al., 2008) for a garnet-bearing Uspensky granite. In addition, Sakhno et al. (2016) reported a 107.1 ± 1.3 Ma SHRIMP age for a granite within the Priiskovy massif (Biser complex).

The granitoids of the Tatiba series contain tungsten-bearing skarns and greisens (Gvozdev, 2010; Solovev, 1995). The age of mineralization is ca. 110–105 Ma.

2.4. Cenomanian–Maastrichtian igneous episode (95–65 Ma)

The Cenomanian–Maastrichtian development of the Sikhote-Alin area was dominated by Andean-type active continental margin tectonics and magmatism, exemplified by the formation of the East Sikhote-Alin volcanic belt (ESAVB). Here, we focus on the plutonic rocks within this belt, specifically the Ol'ga and Dal'negorsk granitoids within the Ol'ga magmatic series.

2.4.1. Ol'ga granitoids

The Santonian–Campanian Ol'ga granitoids are a discontinuous band of intrusive rocks that crop out along the Sea of Japan coastline (Fig. 2c), with isolated intrusive bodies also cropping out to the east of the Central Fault zone. Petrologically, geochemically, and structurally, these granitoids are closely related to the Late Cretaceous volcanic rocks.

Individual intrusions within the complex vary in size from small stocks and dikes to batholiths of hundreds of square kilometers in area. Large intrusions within the complex are usually two-phase, with an initial diorite (rarely gabbro–diorite) phase superseded by a second phase of granite and quartz-diorite. These intrusions are sheet-like bodies (up to 2 km thick), with their upper sections hosted in Late Cretaceous felsic volcanic rocks and lower sections in terrigenous sediments of the Taukha accretionary prism that underlies the volcanic units (Valuy, 2014). The diorites within this complex have a plagioclase–hornblende–biotite–pyroxene–quartz–alkali feldspar paragenetic sequence, whereas the quartz-diorites are pyroxene free and contain more biotite than hornblende. The opposite (i.e., a predominance of hornblende over biotite) is true of the diorites. The majority of the granites in the complex are biotite bearing, pyroxene free, and contain rare and heterogeneously distributed hornblende (Valuy and Strizhkova, 1997).

The granitoids are acidic to moderately acidic, and moderately to highly alkaline, with K₂O concentrations of 2.5–5.0 wt.% and Na₂O concentrations of 2.7–4.5 wt.% (Valuy, 2014; Valuy and Strizhkova, 1997). The Shand A/CNK values of these rocks indicate that the majority are metaluminous, although the most fractionated granites (SiO₂ > 73 wt.%) are peraluminous. The highest A/CNK values may be indicative

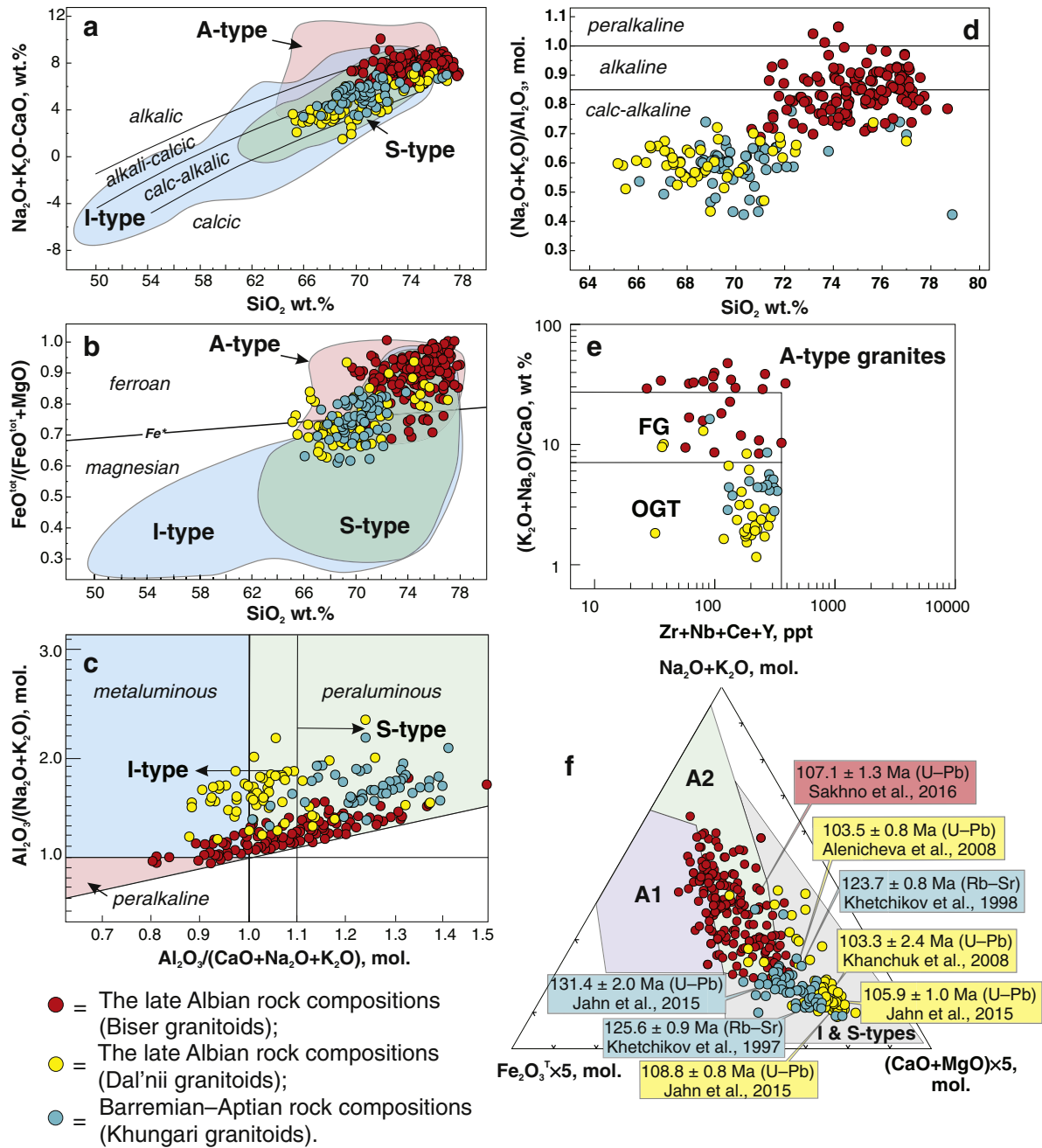


Fig. 3. Geochemical discrimination diagrams: (a) variations in $\text{Na}_2\text{O} + \text{K}_2\text{O}$ vs. CaO against SiO_2 showing the approximate ranges for alkalic, alkali-calcic, calc-alkalic, and calcic-alkali samples including the fields for A-, S-, and I-type rocks (Frost et al., 2001). (b) $\text{FeO} / (\text{FeO} + \text{MgO})$ vs. SiO_2 (in wt.%) diagram showing the boundary between ferroan and magnesian silicic rocks and fields for A-, S-, and I-type rocks; the Fe-number line is defined as $\text{FeO} / (\text{FeO} + \text{MgO}) = 0.446 + 0.0046 \times \text{SiO}_2$ (in wt.%; Frost et al., 2001). (c) A/NK ($\text{Al}_2\text{O}_3 / \text{Na}_2\text{O} + \text{K}_2\text{O}$) vs. A/CNK ($\text{Al}_2\text{O}_3 / \text{CaO} + \text{Na}_2\text{O} + \text{K}_2\text{O}$, all in molar quantities) diagram of Shand's index (Maniar and Piccoli, 1989). (d) Agpaic index ($\text{Na}_2\text{O} + \text{K}_2\text{O} / \text{Al}_2\text{O}_3$ (in molar quantities; Liégeois and Black, 1987). (e) $\text{Zr} + \text{Nb} + \text{Ce} + \text{Y}$ vs. $(\text{Na}_2\text{O} + \text{K}_2\text{O}) / \text{CaO}$ discrimination diagram for A-type granites showing fields for fractionated felsic granites (FG) and non-fractionated M-, I-, and S-type granites (OGT; Whalen et al., 1987). (f) Variations in $(\text{Na}_2\text{O} + \text{K}_2\text{O})$ vs. $\text{Fe}_2\text{O}_3 \times 5$ vs. $(\text{CaO} + \text{MgO}) \times 5$ (in molar quantities; Grebennikov, 2014).

of crustal contamination, as suggested by White et al. (1986). Most of the granitoids are I-type granites, with a few being S-type (Fig. 4c), and they are predominantly calc-alkaline, ferroan, and magnesian, although some of the more evolved granitoids ($\text{SiO}_2 > 73$ wt.%) are calcic (Fig. 4a–e).

The majority of these granitoids formed in a volcanic arc setting, according to the tectonic discrimination diagram of Pearce et al. (1984). The spidergrams for these rocks show depletions, or negative anomalies, in Nb–Ta, Sr, P, Zr, and Ti (Jahn et al., 2015). Negative Ti–Nb–Ta anomalies are characteristic of granitic rocks, island arc volcanic rocks, and the continental crust in general. The Zr, Nb, Ce, and Y concentrations of these samples indicate that they are orogenic granitoids or highly

differentiated quartz–feldspathic granitoids according to the diagrams of Whalen et al. (1987; Fig. 4e). These granitoids are also characterized by relatively low initial Sr ratios (0.7047–0.7074) and slightly negative ε_{Nd} values (−1.05 to −3.61; Valui and Moskalenko, 2010). The Sr–Nd–Hf isotopic data suggest that the granitoids were generated by partial melting of sources with significant proportions of subducted oceanic basalt or underplated basaltic magma, together with continental crust components (Jahn et al., 2015).

The timing of intrusion of the Ol'ga granitoids is constrained by their sharp contacts with the Turonian–Campanian felsic volcanic rocks and the fact that they are overlain by Maastrichtian–Danian volcanic rocks. K–Ar dating of these intrusions has yielded ages of 88–41 Ma

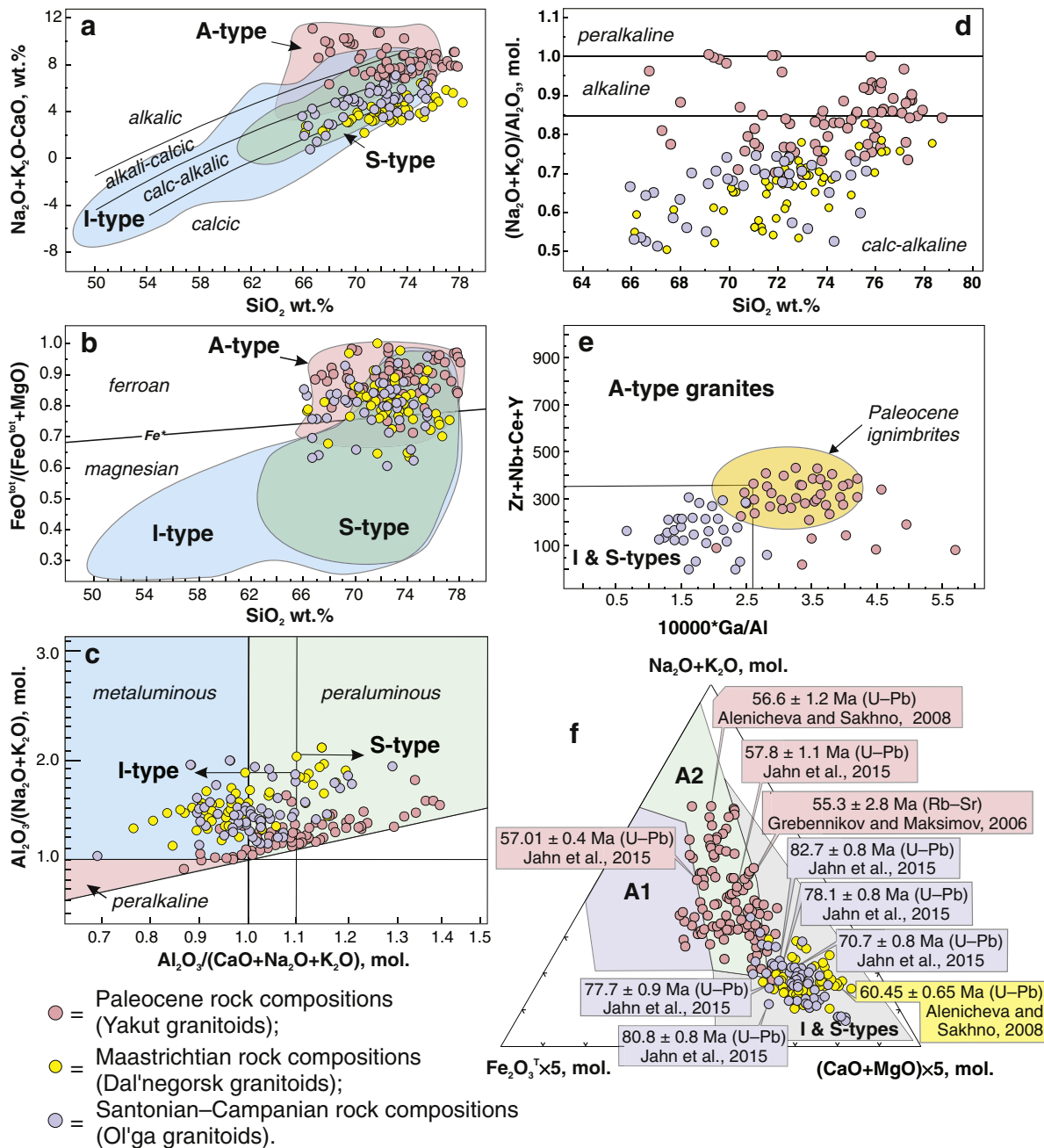


Fig. 4. Geochemical discrimination diagrams: (a) variations in $\text{Na}_2\text{O} + \text{K}_2\text{O}$ vs. CaO against SiO_2 showing approximate ranges for alkalic, alkali-calcic, calc-alkalic, and calcic-alkali compositions and the fields of A-, S-, and I-type rocks (Frost et al., 2001). (b) $\text{FeO} / (\text{FeO} + \text{MgO})$ vs. SiO_2 (in wt.%) diagram, including the boundary between ferroan and magnesian silicic rocks and the fields of A-, S-, and I-type rocks; the Fe-number line is defined by $\text{FeO} / (\text{FeO} + \text{MgO}) = 0.446 + 0.0046 \times \text{SiO}_2$ (in wt.%; Frost et al., 2001). (c) A/NK ($\text{Al}_2\text{O}_3 / \text{Na}_2\text{O} + \text{K}_2\text{O}$) vs. A/CNK ($\text{Al}_2\text{O}_3 / \text{CaO} + \text{Na}_2\text{O} + \text{K}_2\text{O}$, all in molar quantities) diagram of Shand's index (Maniar and Piccoli, 1989). (d) Agpaite index ($(\text{Na}_2\text{O} + \text{K}_2\text{O}) / \text{Al}_2\text{O}_3$ (in molar quantities; Liégeois and Black, 1987). (e) $\text{Zr} + \text{Nb} + \text{Ce} + \text{Y}$ vs. $10,000 \times \text{Ga} / \text{Al}$ discrimination diagram for A-type granitoids; I and S-type fields are from Whalen et al. (1987). (f) Variations in $(\text{Na}_2\text{O} + \text{K}_2\text{O})$ vs. $\text{Fe}_2\text{O}_3 \times 5$ vs. $(\text{CaO} + \text{MgO}) \times 5$ (in molar quantities; Grebennikov, 2014).

(e.g., Baskina (1982) and Khanchuk (2006)), whereas zircon U–Pb dating of a second-phase granite within the complex yielded an age of 82.7–70.4 Ma (Jahn et al., 2015).

2.4.2. Dal'negorsk granitoids

The Maastrichtian Dal'negorsk granitoids are a granite–diorite complex of small and poorly differentiated ilmenite-bearing magmatic bodies within an area between the Sea of Japan and the Central Sikhote-Alin Fault zone (Fig. 2c). The intrusions consist of multiple phases but typically follow the same developmental succession, from an initial phase of diorite, gabbro–diorite, and monzonite to a second phase of quartz–diorite and quartz–monzonite, a third phase of granite, porphyritic

granite, and quartz–diorite, and a final stage of emplacement marked by widespread diiking. The presence of granophyric and porphyritic textures indicates that the intrusions solidified at shallow depths. The granitoids are ubiquitously associated with hornfelsing of Triassic–Jurassic and Lower Cretaceous sediments of the Taukha and Kema terranes and Upper Cretaceous volcanic rocks (Valuy, 2014; Valuy and Strizhkova, 1997). The diorites within this complex have a plagioclase–hornblende–biotite–pyroxene–quartz–alkali feldspar paragenetic sequence, whereas the quartz–diorites contain plagioclase, quartz in higher abundances than alkali feldspar, hornblende, and biotite. The majority of granites in the complex have an alkali feldspar–quartz–plagioclase paragenetic sequence and are hornblende bearing.

The accessory minerals are apatite, zircon, ilmenite, and allanite (Valuy, 2014).

All of the units within the Dal'negorsk complex is characterized by normal alkalinities with K_2O and Na_2O concentrations of 1.4–4.7 and 2.5–3.9 wt.%, respectively. The gabbros and diorites within the complex typically have higher alkalinities, a feature that is confirmed by mineralogy. The concentrations of alkaline elements do not vary as a function of alumina content. Na concentrations are always higher than K concentrations in all but the most evolved rocks, which have similar amounts of both elements. The Shand A/CNK values (Shand, 1943) of most of these rocks indicate that they are metaluminous, with a few samples classified as peraluminous. The Dal'negorsk granitoids are classified as I-type granites, with only the Partizansky massif granitoids being classified as S-type granites (Fig. 4c). These rocks are also calcic, ferroan, and magnesian, according to the classification diagrams of Frost et al. (2001; Fig. 4a–b), and they plot in the volcanic arc field of the tectonic discrimination diagram of Pearce et al. (1984). In addition, these samples have Zr, Nb, Ce, and Y concentrations indicative of orogenic granitoids (Whalen et al., 1987), barring samples with the lowest SiO_2 concentrations, which plot in the fractionated granite (FG) field. These also have rather low initial Sr values (0.7032–0.7061) and slightly negative ϵ_{Nd} values (–0.89 to –0.98; Valuy and Moskalenko, 2010).

The Maastrichtian age of the complex is proposed because these intrusions cross-cut the Late Cretaceous felsic volcanic rocks and are overlain by younger Paleocene–Eocene basalts. The granitoids also yield highly variable K–Ar ages of 71–63 Ma (Baskina, 1982; Belyansky et al., 2011), whereas the diorites yield a weighted mean zircon U–Pb age of 60.45 ± 0.65 Ma (Alenicheva and Sakhno, 2008).

Mineralization in the Cenomanian–Maastrichtian granitoids is heterogeneously developed, dominated by tin–polymetallic mineralization (80–65 Ma; Gonevchuk, 2002; Gonevchuk et al., 2010). The polymetallic deposits of Partizanskoe, Nikolaevskoe, and Verkhnee are characteristic of the Dal'negorsk granitoids. These lead–zinc–silver skarn ores formed in contact zones with Late Cretaceous volcanic rocks (Khanchuk, 2006; Simanenko and Ratkin, 2008). Separate ore bodies occur in pre-ore (75–50 Ma) basalt dykes that are cut by post-ore porphyritic dykes (66–57 Ma).

2.5. Paleocene igneous episode (60–45 Ma)

The Paleocene evolution of the Sikhote-Alin area is dominated by magmatic maxima in the outermost western zone of the ESAVB, the formation of large sub-latitude volcanic depressions containing Paleocene volcanic rocks, and the emplacement of an intrusive series (herein referred to as the Yakut granitoids; Fig. 2d).

2.5.1. Yakut granitoids

The Yakut granitoids consist of a series of leucocratic granite, alkali-feldspar-granite, and porphyritic granite intrusions that are genetically related to Paleocene acid volcanic rocks, which explains why these intrusions are spatially limited to the volcanic fields of the East Sikhote-Alin area. The sheet-like granitoid bodies intrude between volcanic strata, sealing off volcanic conduits and dikes, and fill ring and radial faults within volcanic depressions. Almost all of these intrusions are associated with subvolcanic endocontact zones that contain highly porphyritic rocks with poorly crystallized felsic, spherulitic, or axiolitic matrixes. The textural similarities of the intrusive and extrusive rocks in the study area suggest that all of the Yakut granitoids are subvolcanic rocks that formed at depths of several hundred meters.

The Yakut rocks are primarily alkali-feldspar-granites and leucogranites, rarer aegirine-riebeckite granites, and quartz-syenites. The former two types have phenocrysts that consist predominantly of oligoclase (up to 40% modal abundance), quartz, perthitic alkali feldspar, and hypersthene, and more rarely of magnetite, augite, hornblende, and biotite. The aegirine-riebeckite granites are fine-grained, porphyritic, or pegmatitic rocks that contain variable proportions of quartz, alkali

feldspar, albite, aegirine, and riebeckite. Accessory minerals are predominantly zircon, xenotime, and bastnaesite, and more rarely columbite and chevkinite (Belyansky et al., 2011; Mikhailov, 1989). All of these intrusions are potassium rich and have high concentrations of iron at low to moderate degrees of oxidation. They have SiO_2 concentrations of typically 70–73 wt.%, and up to 76 wt.% in the most acidic intrusions (Mikhailov, 1989). The vast majority of these rocks are peraluminous, although rare examples are peralkaline (Fig. 4c). These intrusions are calc-alkalic to alkalic, are predominantly ferroan (Fig. 4a–d), plot in an intermediate position between the volcanic arc and within-plate granite fields on the tectonic discrimination diagram of Pearce et al. (1984), and are A-type granites on the classification diagram of Whalen et al., 1987 (Fig. 4e). The classification diagrams indicate that the granitoids of the Yakut series formed in A2-granite-type intracontinental and continental-margin geodynamic settings (Grebennikov, 2014; Fig. 4f), or as post-collisional, post-orogenic, and anorogenic granitoids that formed from island arc basalts (IAB) and continental-margin basalts, from crustal tonalites and granodiorites, or through the partial melting of crust (Eby, 1992). These intrusions are characterized by high concentrations of large ion lithophile elements (LILEs), high field strength elements (HFSEs; e.g., Nb, Ga, and Y), rare earth elements (REEs; barring Eu), and low Sr and Sc concentrations. They also have fractionated REE patterns relative to those of typical upper continental crust, with La_N/Yb_N values of 3.2–10.2 and Eu/Eu^* values of 0.1–0.7 (Grebennikov and Maksimov, 2006).

The Paleocene age of these granitoids is inferred from sharp contacts with Maastrichtian–Paleocene volcanic rocks and the fact that some of these intrusive bodies are overlain by Eocene basalts. The granites yield a Rb–Sr internal isochron age of 55.3 ± 2.8 Ma ($^{87}Sr/^{86}Sr_i = 0.70692 \pm 0.00035$; Grebennikov and Maksimov, 2006) and a weighted mean U–Pb age of 56.6 ± 1.2 Ma (Alenicheva and Sakhno, 2008). These ages are comparable to the age of the youngest dated Paleocene ignimbrite (Grebennikov and Maksimov, 2006).

The Paleocene rhyolite–granite group does not show a consistent pattern of mineralization. Gold–silver porphyry-type mineralization is the most typical style and this is commonly associated with molybdenum and copper mineralization, and more rarely with tin mineralization (Khanchuk, 2006; Popov and Grebennikov, 1997).

3. Discussion

3.1. Summary model of the paleogeodynamic evolution of the Sikhote-Alin area

The Sikhote-Alin section of the Pacific margin is a unique area with a complex geodynamic history. The available geological, geophysical, and petrological data indicate alternating periods of subduction and transform strike-slip movement. During the period 130–45 Myr, after the completion of Jurassic–Early Cretaceous terrane accretion, the geodynamic regime changed repeatedly. In late Albian times, the Sikhote-Alin area was a transform continental margin; then during the Cenomanian–Maastrichtian, it was an active Andean-type margin. During the Paleocene–Eocene, the setting changed back to a transform continental margin, the evolution of which resulted in the opening of the Sea of Japan basin. This sequence resulted in the generation of several granitoid series that are characterized by different ages, compositions, and tectonic settings: the Khungari, Dal'nii, Biser, Ol'ga, Dal'negorsk, and Yakut granitoids.

Two stages of orogeny have been identified in the Sikhote-Alin area in Early Cretaceous. The first stage (Hauterivian–Aptian) was associated with the displacement of the Bureya–Khanka back-arc transform continental margin, which resulted in the deformation of the Sikhote-Alin terranes along the margins of continental blocks due to activity on the Tan–Lu fault system. This displacement caused sedimentary masses to crumple into systems of closely pressed folds with near-horizontal fold axes, often in combination with thrusting (Khanchuk et al., 2004).

Consequently, the base of this sedimentary sequence reached sufficient temperatures and pressures to allow partial melting, thereby generating the first phase of the Early Cretaceous anatectic S-type melts of the Khungari granitoids (Fig. 5a), all of which are restricted to the cores of large-scale folds with subvertical flexures and are associated with anomalously wide (up to 1.5 km) aureoles of cordierite–biotite and biotite hornfels, located above the roof zones of the granite intrusions (Izokh et al., 1967; Sakhno, 2001; Simanenko et al., 1997).

The second stage (late Albian) involved continued horizontal compression caused by movement of the Izanagi Plate along the continental margin of Asia (Maruyama et al., 1997), which led to the collision of the Kema island arc with Zhuravlevka–Amur terrane (e.g., Golozubov, 2006; Golozubov and Lee, 1997; Lee, 1999; Lee and Paik, 1990; Utkin, 1985). Large-scale translations from south to north along the

continental margin, in combination with left-lateral strike-slip displacements, led to folding of the terranes. The Jurassic accretionary prism and the Early Cretaceous Zhuravlevka–Amur and Kema terranes to were deformed into an “S” shape, producing a giant vertical fold and oroclinal bending (Golozubov, 2006; Khanchuk et al., 2004). The deformation caused the rapid thickening of the crust in this area, the generation of a metamorphosed granite layer, and the formation of numerous syn-faulting extensional or compressional basins accompanied by the injection of voluminous granitoid magmas (Tatiba series), marking the end of the formation of new continental lithospheric crust (Khanchuk et al., 2013; Fig. 5b). This tectonism indicates that the Sikhote-Alin area at this time was a typical transform continental margin, with the proto-Central Sikhote-Alin Fault and its extensions into Japan (the Tanakura and Median faults) subsequently inheriting the lithospheric

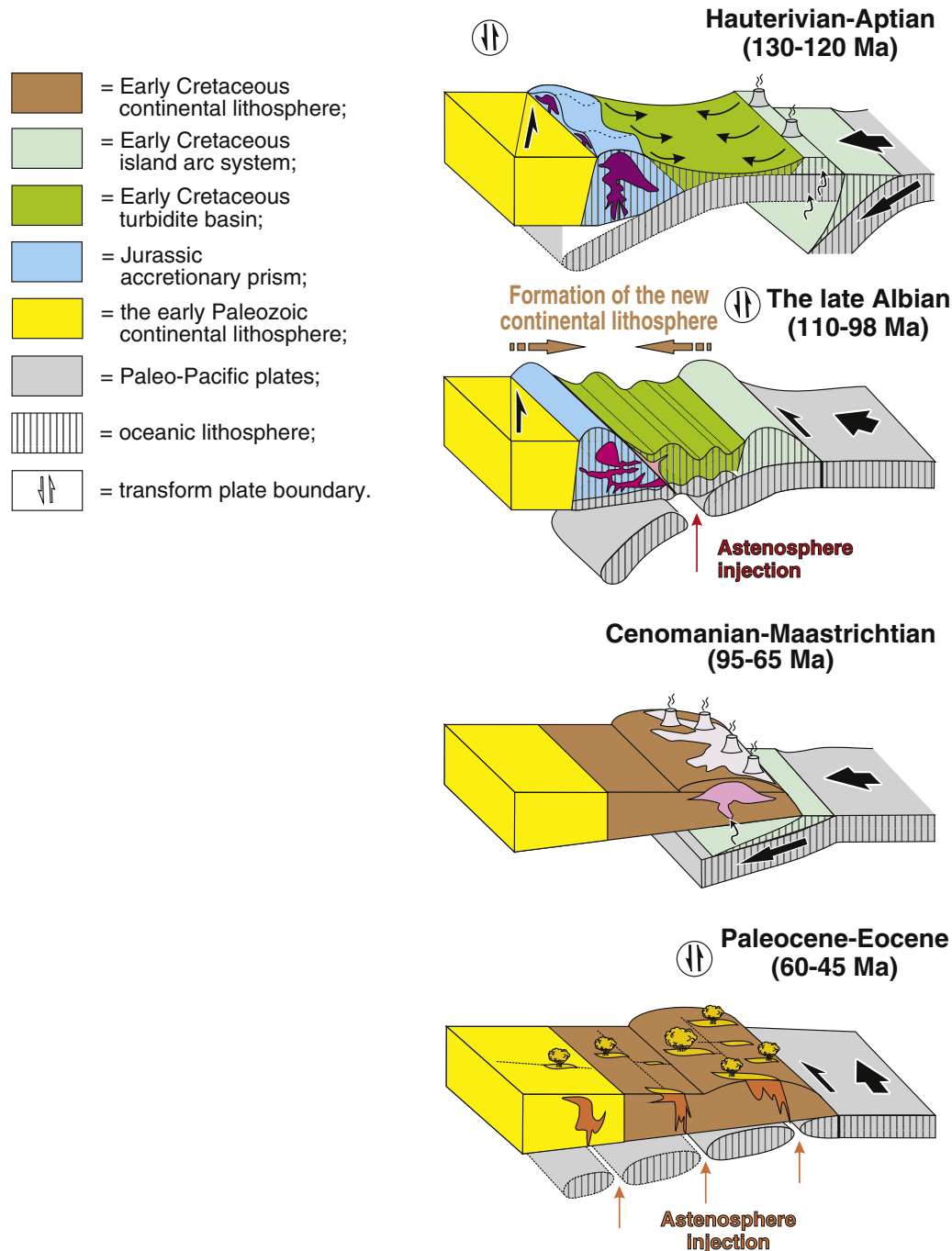


Fig. 5. Model showing a paleogeodynamic reconstruction of the Sikhote-Alin area.

plate boundary in a similar fashion to the present-day San Andreas Fault in California (Khanchuk, 2001). The existence of a transform continental margin in the Sikhote-Alin area is confirmed by comprehensive tectonic, geodynamic, seismic, magmatic, and mineralization data and is exemplified in the initiation of the Tan–Lu fault system along the continental plate margin, termination of the formation of the Jurassic subduction accretionary prism, and genesis of the Early Cretaceous Zhuravlevka–Amur turbidite basin along the plate boundary (Golozubov, 2006; Kemkin, 2012; Khanchuk, 2001). There exists no evidence for subduction beneath the Sikhote-Alin area at the end Albian (Khanchuk, 2001, 2006; Khanchuk et al., 1997). This is supported by the similar ages of picrite–alkali basalt association of the Dayansky complex within the Badzhal terrane (Maksimov et al., 2001), the intrusion of several plutons that host gabbro–monzonites in the southern Zhuravlevka–Amur terrane close to the Central Fault (Gonevchuk, 2002; Gonevchuk et al., 2011), and the emplacement of trachybasalts and trachyandesites related to mantle-derived magmas (Simanenko et al., 2002). Interaction between ascending asthenospheric diapirs and the accretionary wedge resulted in the generation of mantle-derived alkaline–subsilicic magmas. This magmatism induced intensive melting of the metapelites and more refractory crustal material in this area (e.g., metamorphosed oceanic basalts present as enclaves within and beneath the accretionary wedge), generating the coeval Biser (A-type) and Dal'nii (S- and I-type) granitoids. The compositions of the Biser granitoids indicate that these rocks formed from magmas generated at high temperatures and under conditions of low oxygen fugacity, indicating a mantle origin (Khanchuk, 2006, and references therein). The compositions of the Dal'nii granitoids are the result of mixing of anatectic melts, derived from the melting of metapelites, plus minor melts of metabasites (mainly depleted, similar to N-MORB), which formed at 8 kbar in the presence of water (Kruk et al., 2014). This relationship with the Pacific margin of the Far East of Russia in areas of compression-dominated tectonism and strike-slip movements was explained by Golozubov (2006), who suggested that the different orientations of the margin were affected by the northward movement of the Izanagi Plate, which led to correspondingly different angles of convergence. This movement (in late-collisional and post-collisional settings) resulted in localized transpressional and transtensional deformation.

The Cenomanian–Maastrichtian (95–70 Ma) tectonic setting of the East Asian margin was similar to that of the present day, with northwestward movement of the Izanagi Plate at 100–85 Ma and westward movement of the same plate at 85–74 Ma (Engelbreton et al., 1985), leading to the initiation of frontal subduction. This resulted in the generation of the East Asia volcanic belt within the continental margin of Asia. This magmatism was an Andean-type event that generated Late Cretaceous plateau-forming ignimbrites and their Santonian–Campanian (Ol'ga) intrusive analogs, followed by Maastrichtian (Dal'negorsk) granitoids (Fig. 5c). The compositions of these magnesian–ferrous, calcic, and calcic–alkali rocks indicate that they formed from metaluminous (or peraluminous for the volcanic derivatives) I-type felsic magmas. These melts were generated by the partial melting of metasedimentary and metamagmatic rocks in an oxidized and water-containing environment that typifies volcanism in supra-subduction geodynamic settings (Grebennikov and Popov, 2014; Jahn et al., 2015; Simanenko and Khanchuk, 2003).

Engelbreton et al. (1985) suggested that tectonism during the Maastrichtian–Paleocene (70–55 Ma) followed the accretion of terranes to North Asia and was characterized by movement of the Pacific Plate to the northwest, at a distinct angle to the continental margin. This complex plate interaction resulted in the coexistence of contemporaneous active and transform margin tectonism within different areas of the same margin. Areas dominated by displacement along the Pacific Plate were associated with sinistral transform margin development, whereas areas dominated by the displacement of the North American (and the Okhotsk Sea) plates along the boundary with Eurasia (e.g., along the Hokkaido–Sakhalin fault system) underwent dextral strike-slip deformation.

Paleocene–Eocene magmatism in the study area commenced after the termination of active subduction in a rifting regime related to strike-slip movement of the oceanic plate relative to the continent (Khanchuk et al., 1997). The Yakut granitoids were emplaced during this time, and their volcanic analogs (Grebennikov and Popov, 2014) are typical of A-type rocks. A-type granites and rhyolites are usually associated with mantle-derived melts and reduced fluids, which form in a zone undergoing extension (e.g., Dall'Agnol et al. (2012) and Martin (2006)). These Rb-, REE-, Y-, and Th-rich, calc-alkalic to alkalic, peraluminous rocks are found worldwide, including in the continental-scale Central Asian Orogenic Belt (CAOB; e.g., Bonin (2007); Frost and Frost (2011) and Wu et al. (2002)). They form at times of a global change in geodynamic setting, and the orthogonal (counter) movement of plates at a convergent boundary (subduction) gives way to shear relative to each other, i.e., a transform continental margin setting (Khanchuk et al., 1997). In this case, the subsided slab (i.e., that part of the plate has entered the subduction zone) and the oceanic plate (outboard of the subduction zone) will have different dynamic characteristics because of their locations at different hypsometric levels. Therefore, at depths of no greater than a few tens of kilometers, the slab may break to form steeply inclined structures of shear extension, which provide pathways for ascending mantle material. Zones of transform faults that have subducted beneath the active continental margin are the most favorable structures for the formation of feeder zones for ascending mantle material (Fig. 5d). Paleocene alkaline ultrabasic volcanic rocks, fayalite rhyolites, and coeval intrusions of gabbro and syenite are another characteristic feature of the Sikhote-Alin (Grebennikov and Maksimov, 2006; Kazachenko et al., 2013; Mikhailov, 1989). These features are comparable with those of the classic examples of transform continental margins (e.g., the west of Northern America).

Basaltic and bimodal volcanism began in the Sikhote-Alin and at the margin of the Khanka terrane in the early Eocene (55 Ma) and lasted until the opening of the Sea of Japan was complete (ca. 15 Ma). The eruption of Eocene–Oligocene–early Miocene peraluminous basalts corresponded to upwelling of hot depleted oceanic asthenosphere of the Pacific MORB-type into Asian subcontinental lithosphere with EMII-like isotopic characteristics. The interaction of the Pacific asthenosphere with subcontinental lithosphere (EMII) could only occur after the destruction of the subducted slab and the formation of a slab window (Martynov and Khanchuk, 2013).

4. Conclusions

- i. The Sikhote-Alin section of the Pacific margin is a peculiar area with a complex geodynamic history. The available stratigraphic, metamorphic, and geochronological data indicate alternating periods of subduction and transform strike-slip movement of oceanic plates. This sequence resulted in the generation of several granitoid suites that are characterized by different ages, compositions, and tectonic settings.
- ii. The first, Early Cretaceous (Hauterivian–Aptian: 130–120 Ma) orogenic stage, associated with the displacement of the Bureya–Khanka continental margin, resulted in the deformation of the Jurassic accretionary prism and Early Cretaceous turbidite basin along faults of the Tan–Lu system. This deformation caused a rapid thickening of the crust in this area and the generation of the earliest anatectic peraluminous (two-mica, cordierite-bearing) granitoids of the Sikhote-Alin.
- iii. In the second (late Albian: 110–98 Ma) stage of tectonism, the Sikhote-Alin area was a transform continental margin. The collision of the Kema island arc with the continental margin led to the continued deformation of epi-oceanic terranes, the break-off of the subducted plate, and the injection of oceanic asthenospheric material into the slab window. This marked the end of the period of formation of new continental crust, led to the generation of a metamorphosed granite layer, and resulted in the injection of voluminous magmas

- of calc-alkaline magnesian (S- and I-type) and alkali-calcic ferroan (A-type) granitoids into syn-faulting compressional and extensional basins, respectively. Coeval intrusions that host gabbro–monzonites and trachybasalts–trachyandesites are evidence of the close relationship between A-type rocks and mantle-derived magmas that intruded the transtensional deformation zones.
- iv. Northwestward to westward movement of the Izanagi Plate resulted in the initiation of frontal subduction of the Paleo-Pacific Plate (95–70 Ma). In turn, this resulted in the generation of the Late Cretaceous East Asia volcanic belt within the Asian continental margin. This magmatism was an Andean-type event that generated Late Cretaceous plateau-forming ignimbrites and their Santonian–Campanian intrusive analogs, followed by Maastrichtian granitoids. The compositions of these magnesian–ferrous, calcic to calc-alkaline rocks indicate that they formed from metaluminous I-type felsic magmas.
 - v. Paleocene–Eocene magmatism (60–45 Ma) in the Sikhote-Alin area commenced after the termination of subduction in a rifting regime related to strike-slip movement of the oceanic plate relative to the continent. The break-off of the subducted plate and the injection of oceanic asthenospheric material into the subcontinental lithosphere resulted in the eruption of alkaline ultrabasic rocks, fayalite rhyolites, and coeval intrusions of gabbro, syenite and alkali feldspar granites (A-type). The rifting evolution of continental lithosphere resulted in the opening of the Sea of Japan basin.
 - vi. The A-type granitoids and coeval gabbro–monzonites of the Sikhote-Alin area formed in a geodynamic setting comprising transform strike-slip movements of oceanic and continental lithospheric plates and are considered to be reliable indicators of this paleotectonic environment.

Acknowledgments

The authors would like to thank G. Nelson Eby, Bernard Bonin, Boris A. Litvinovsky, and anonymous reviewers for their helpful suggestions that improved the presentation of this paper.

This work was supported by the Russian Foundation for Basic Research grant 13-05-12090 OFI_M.

Appendix A. Supplementary data

Supplementary data to this article can be found online at <http://dx.doi.org/10.1016/j.lithos.2015.12.020>.

References

- Alenicheva, A.A., Sakhno, V.G., 2008. The U–Pb dating of extrusive-intrusive complexes in ore districts in the southern part of the Eastern Sikhote-Alin Volcanic Belt. *Doklady Earth Sciences* 419 (2), 217–221 (in Russian).
- Alenicheva, A.A., Sakhno, V.G., Saltykova, T.E., 2008. U–Pb and Rb–Sr dating of granitoids from the Tatibin Group in the plutonic belt of Central Sikhote-Alin. *Doklady Earth Sciences* 420 (4), 533–537.
- Baskina, V.A., 1982. *Magmatism of Ore-controlling Structures of Primorye*. Nauka, Moscow (in Russian).
- Belyansky, G.S., Rybalko, V.I., Syas'ko, A.A., Bazhanov, V.A., Uglova, N.I., Abramova, V.A., Ole'nikov, A.V., Kovalenko, S.V., Kashtaev, B.I., Alenicheva, A.A. and Gonokhova, N.G. (Eds.), 2011. State Geological Map of Russian Federation. Scale 1: 1000000 (third edition). Sheet (L–52), 53; (K–52), 53) – Khanka Lake. Explanatory note. Cartographic factory of A.P. Karpinsky Russian Geological Research Institute, St. Petersburg, (in Russian).
- Bonin, B., 2007. A-type granites and related rocks: evolution of a concept, problems and prospects. *Lithos* 97, 1–29.
- Chappell, B.W., White, A.J.R., 1974. Two contrasting granite types. *Pacific Geology* 8, 173–174.
- Cheng, R.Y., Wu, F.Y., Ge, W.C., Sun, D.Y., Yang, J.H., 2006. Emplacement age of the Raohe Complex in eastern Heilongjiang Province and the tectonic evolution of the eastern part of northeastern China. *Acta Petrologica Sinica* 22, 353–376 (in Chinese with English abstract).
- Dall'Agnol, R., Frost, C.D., Rämö, O.T., 2012. IGCP project 510 “A-type granites and related rocks through time”: project vita, results, and contribution to granite research. *Lithos* 151, 1–16.
- Eby, G.N., 1992. Chemical subdivision of the A-type granitoids: petrogenetic and tectonic implications. *Geology* 20 (7), 641–644.
- Engelbreton, D., Cox, A., Gordon, R.G., 1985. Relative motions between oceanic and continental plates in the northern Pacific basin. *Geological Society of America Special Papers* 206, 1–59.
- Faure, M., Nataf'in, B., 1992. The geodynamic evolution of the eastern Eurasian margin in Mesozoic times. *Tectonophysics* 208 (4), 397–411.
- Frost, C.D., Frost, B.R., 2011. On ferroan (A-type) granitoids: their compositional variability and modes of origin. *Journal of Petrology* 52 (1), 39–53.
- Frost, B.R., Barnes, C.G., Collins, W.J., Arculus, R.J., Ellis, D.J., Frost, C.D., 2001. A geochemical classification for granitic rocks. *Journal of Petrology* 42 (11), 2033–2048.
- Golozubov, V.V., 2006. Tectonics of the Jurassic and Lower Cretaceous Complexes of the North-Western Framing of the Pacific Ocean. *Dal'nauka, Vladivostok* (in Russian).
- Golozubov, V.V., Lee, D.W., 1997. Dynamics of formation of the Early Cretaceous Partizansk–Sukhodol epicontinental basin (South Primorye). *Russian Journal of Pacific Geology* 16 (6), 46–57 (in Russian).
- Gonevchuk, V.G., 2002. Magmatism and Metallogenesis of Tin-Bearing Systems of the Russian Far East. *Dal'nauka, Vladivostok* (in Russian).
- Gonevchuk, V.G., Gonevchuk, G.A., Korostelev, P.G., Semenyak, B.I., Seltmann, R., 2010. Tin deposits of the Sikhote-Alin and adjacent areas (Russian Far East) and their magmatic association. *Australian Journal of Earth Sciences* 57, 777–802.
- Gonevchuk, V.G., Gonevchuk, G.A., Lebedev, V.A., Orekhov, A.A., 2011. Monzonitoid association of the Kavalerovo Ore District (Primorye): geochronology and some genetic problems. *Russian Journal of Pacific Geology* 5 (3), 199–209.
- Grebennikov, A.V., 2014. A-type granites and related rocks: petrogenesis and classification. *Russian Geology and Geophysics* 55 (11), 1353–1366.
- Grebennikov, A.V., Maksimov, S.O., 2006. Fayalite rhyolites and a zoned magma chamber of the Paleocene Yakutinsky volcanic depression in Primorye, Russia. *Journal of Mineralogical and Petrological Sciences* 101 (2), 69–88.
- Grebennikov, A.V., Popov, V.K., 2014. Petrogeochemical aspects of the Late Cretaceous and Paleogene ignimbrite volcanism of East Sikhote-Alin. *Russian Journal of Pacific Geology* 8 (1), 38–55.
- Gvozdev, V.I., 2010. Ore-Magmatic Systems of Skarn Scheelite-Sulfide Deposits in Eastern Russia. *Dal'nauka, Vladivostok* (in Russian).
- Ivanov, B.S., Bur'yanova, I.Z., Zalizhchak, B.P., Stepanov, G.N., 1980. Granitoids and monzonitoids of Ore Districts of Primorye. Nauka, Moscow (in Russian).
- Izokh, E.P., Russ, V.V., Kunaev, I.V., Nagovskaya, G.N., 1967. Ore Content and Origin of Intrusive Bodies of the Northern Sikhote-Alin. Nauka, Moscow (in Russian).
- Jahn, B.-M., Valui, G., Kruk, N., Gonevchuk, V., Usuki, M., Wu, J.T.J., 2015. Emplacement ages, geochemical and Sr–Nd–Hf isotopic characterization of Mesozoic to early Cenozoic granitoids of the Sikhote-Alin Orogenic Belt, Russian Far East: crustal growth and regional tectonic evolution. *Journal of Asian Earth Sciences* 111, 872–918.
- Kazachenko, V.T., Khanchuk, A.I., Lavrik, S.N., Perevoznikova, E.V., 2013. Phlogopite–olivine rocks of the Taukha terrane in southeastern Sikhote-Alin. *Russian Journal of Pacific Geology* 7 (5), 330–345.
- Kemkin, I.V., 2008. Structure of terranes in a Jurassic accretionary prism in the Sikhote-Alin–Amur area: implications for the Jurassic geodynamic history of the Asian eastern margin. *Russian Geology and Geophysics* 49 (10), 759–770.
- Kemkin, I.V., 2012. Microfaunal biostratigraphy and structural framework of the Nadezhda–Bikin terrane within a Jurassic accretionary prism of the Sikhote-Alin Fold Belt, eastern Russia. *Journal of Asian Earth Sciences* 61, 88–101.
- Khanchuk, A.I., 2001. Pre-Neogene tectonics of the Sea-of-Japan region: a view from the Russian side. *Earth Science (Chikyu Kagaku)* 55, 275–291.
- Khanchuk, A.I. (Ed.), 2006. *Geodynamics, Magmatism and Metallogeny of the Russian East*. Dal'nauka, Vladivostok (in Russian).
- Khanchuk, A.I., Ivanov, V.V., 1999. Meso-Cenozoic geodynamic settings and gold mineralization of the Russian Far East. *Russian Geology and Geophysics* 40 (11), 1607–1617.
- Khanchuk, A.I., Kemkin, I.V., 2003. Geodynamic evolution of Japan-Sea region in Mesozoic. *Bulletin of FEBRAS* 6, 99–116 (in Russian).
- Khanchuk, A.I., Ratkin, V.V., Ryazantseva, M.D., Golozubov, V.V., Gonokhova, N.G., 1996. *Geology and Mineral Deposits of Primorsky Krai*. Dal'nauka, Vladivostok.
- Khanchuk, A.I., Golozubov, V.V., Martynov, Yu. A., Simanenkov, V.P., 1997. Early Cretaceous and Paleogene transform continental margins (Californian type) of the Russian Far East. *Tectonics of Asia*. GEOS, Moscow, pp. 240–243 (in Russian).
- Khanchuk, A.I., Golozubov, V.V., Simanenkov, V.P., Malinovsky, A.I., 2004. The large-size folds with steeply inclined axes within orogenic belts structures: exemplified by the Sikhote-Alin region. *Doklady Earth Sciences* 394 (6), 791–795 (in Russian).
- Khanchuk, A.I., Kruk, N.N., Valui, G.A., Nevolin, P.L., Moskalenko, E.Yu., Fugzan, M.M., Kirnozova, T.I., Travin, A.V., 2008. The Uspensk intrusion in South Primorye as a reference petrotype for granitoids of the transform continental margins. *Doklady Earth Sciences* 421 (5), 734–737.
- Khanchuk, I., Kruk, N.N., Golozubov, V.V., Kovach, V.P., Serov, P.A., Kholodnov, V.V., Gvozdev, V.I., Kasatkin, S.A., 2013. The nature of the continental crust of Sikhote-Alin as evidenced from the Nb isotopy of rocks of Southern Primorye. *Doklady Earth Sciences* 451 (2), 809–813.
- Khetchikov, L.N., Govorov, I.N., Pakhomova, V.A., Gerasimov, N.S., Gvozdev, V.I., 1997. The genesis of the Dalninskii complex granitoids in the Sikhote-Alin from isotopic data and the study of inclusions in quartz. *Geology of Pacific Ocean* 13, 227–244.
- Khetchikov, L.N., Pakhomova, V.A., Gvozdev, V.I., Zhuravlev, D.Z., 1998. The isotopic age of granitoids and ores of the Lermontov scarn-scheelite-sulfide deposit of the Central Sikhote-Alin (Russia). *Geology of Ore Deposits* 40 (1), 74–80 (in Russian).
- Krasnyi, L.I., Volskiy, A.S., Vasilieva, I.A., Yumbian, X. and Ying, W. (Eds.), 1996. *Geological Map of Priamurie and Neighboring Territories*. Scale: 1: 2500000. VSEGEI, Amurgeolkom (the Amur Committee on Geology and Mining), Heilongjiang Bureau of Geology and Mineral Resources. (in Russian).
- Kruk, N.N., Simanenkov, V.P., Gvozdev, V.I., Golozubov, V.V., Kovach, V.P., Serov, P.I., Kholodnov, V.V., Moskalenko, E.Yu., Kuibid, M.L., 2014. Early Cretaceous granitoids

- of the Samarka terrane (Sikhote-Alin): geochemistry and sources of melts. *Russian Geology and Geophysics* 55 (2), 216–236.
- Lee, D.W., 1999. Strike-slip fault tectonics and basin formation during Cretaceous in Korean Peninsula. *Island Arc* 8 (2), 218–231.
- Lee, D.W., Paik, K.H., 1990. Evolution of strike-slip fault controlled Cretaceous Yongdong Basin, South Korea: signs of strike-slip tectonics during infilling. *Journal of Geological Society of Korea* 26, 257–276.
- Levashev, G.B., 1991. *Geochemistry of Paragenous Magmatites of Active Continental Margins*. FEB AS USSR, Vladivostok (in Russian).
- Levashev, G.B., Rybalko, V.I., Izosov, L.A., Soroka, V.P., Kovalenko, S.V., Fedchin, F.G., Martynov, Yu. A., Sokarev, A.N., Volosov, A.G., Kulichenko, A.G., Prishchepa, T.K., Semenyak, L.E., Semenova, N.N. (Eds.), 1989. *Tectonomagmatic Systems of Accretionary Crust (the Sikhote-Alin Ridge)*. DVO AN USSR, Vladivostok (in Russian).
- Liégeois, J.P., Black, R., 1987. Alkaline magmatism subsequent to collision in the Pan-African belt of the Adrar des Iforas (Mali). In: Fitton, J.G., Upton, B.J.G. (Eds.), *Alkaline Igneous Rocks*. Geological Society, London, Special Publications 30, pp. 381–401.
- Maksimov, S.O., Moiseenko, V.G., Sakhno, V.G., 2001. High-K basalts of eruptive pipes from the eastern part of the Bureya Massif, Russian Far East. *Doklady Earth Sciences* 379, 640–643.
- Maniar, P.D., Piccoli, P.M., 1989. Tectonic discrimination of granitoids. *Geological Society of America Bulletin* 101, 635–643.
- Martin, R.F., 2006. A-type granites of crustal origin ultimately result from open-system fenitization-type reactions in an extensional environment. *Lithos* 91, 125–136.
- Martinyuk, M.V., Ryamov, S.A., Kondrat'eva, V.A. (Eds.), 1990. *Explanatory Notes for a Plot of Division and Correlation of Magmatic Complexes on the Territories of the Khabarovsk Krai and Amur Region*. Dal'geologiya, Khabarovsk (in Russian).
- Martynov, Yu.A., Khanchuk, A.I., 2013. Cenozoic volcanism of the eastern Sikhote-Alin: petrological studies and outlooks. *Petrology* 21 (1), 85–99.
- Maruyama, S., Isozaki, Y., Kimura, G., Terabayashi, M., 1997. Paleogeographic maps of the Japanese Islands: plate tectonic synthesis from 750 Ma to the present. *The Island Arc* 6, 121–142.
- Mikhailov, V.A., 1989. The Magmatism of Volcanotectonic Structures in the Southern Segments of the East Sikhote-Alin Volcanic Belt. Far East Branch Russian Academy of Science, Vladivostok (in Russian).
- Moskalenko, E.Yu., Kruk, N.N., Valui, G.A., 2011. New geological and geochemical data on the granitoids of the Uspensky massif in Southern Primorye. *Russian Journal of Pacific Geology* 5 (5), 446–457.
- Natal'in, B.A., 1993. History and modes of Mesozoic accretion in Southeastern Russia. *The Island Arc* 2 (1), 15–34.
- Nazarenko, L.F., Bazhanov, V.A. (Eds.), 1987. *Geology of Primorsky Region: In Three Parts*. Far East Geological Institute, Vladivostok (Preprint, in Russian).
- Nokleberg, W.J., Parfenov, L.M., Monger, J.W.H., Norton, I.O., Khanchuk, A.I., Stone, D.B., Scotese, Ch.R., Scholl, D.W., Kazuya, F., 2000. Phanerozoic tectonic evolution of the Circum-North Pacific. U.S. Geological Survey Professional Paper 1626.
- Nokleberg, W.J., Miller, R.J., Naumova, V.V., Khanchuk, A.I., Parfenov, L.M., Kuzmin, M.I., Bounaeva, T.M., Obolenskiy, A.A., Radionov, S.M., Seminskiy, Zh.V., Diggles, M.F., 2003. Project on Mineral Resources, Metallogenesis, and Tectonics of Northeast Asia USGS Open-File Report 03-203. CD-ROM Publication, Menlo Park, California (Internet address: <http://geopubs.wr.usgs.gov/open-file/of03-203>).
- Parfenov, L.M., Khanchuk, A.I., Prokoviev, A.V., Timofeev, V.F., Berzin, N.A., Obolenskiy, A.A., Badarch, G., Tomurtogoo, O., Belichenko, V.G., Dril, S.I., Kuz'min, M.I., Bulgatov, A.N., Kirillova, G.L., Rodionov, S.M., Nokleberg, W.J., Ogasawara, M., Scotese, C.R., Yan, H., 2010. Tectonic and metallogeny model for Northeast Asia. Geological Survey Professional Paper (United States) 1765.
- Pearce, J.A., Harris, N.B.W., Tindle, A.G., 1984. Trace element discrimination diagrams for the tectonic interpretation of granitic rocks. *Journal of Petrology* 25 (4), 956–983.
- Pezhenina, L.A. and Uglov, V.V. (Eds.), 2008. *State Geological Map of Russian Federation*. Scale 1: 1000000. Second edition. The Southern Sikhote-Alin Series. Sheets K-53-III, (Oblachnaya Mnt.) – IV (Olga). Cartographic factory of A.P. Karpinsky Russian Geological Research Institute; St. Petersburg, (in Russian).
- Popov, V.K., Grebennikov, A.V., 1997. Geological and geochemical correlation of Rhyolites from Yakutinsya and Avgustovskaya volcanic structures, Primorie. *Russian Journal of Pacific Geology* 13, 583–600.
- Rub, M.G., Rub, A.K., Akimov, V.M., 1986. Rare-metal bearing granites from the Central Sikhote-Alin. Geological Series of the Proceedings of the USSR Academy of Sciences 7, 33–56 (in Russian).
- Sakhno, V.G., 2001. Late Mesozoic–Cenozoic continental volcanism of East Asia. *Dal'nauka, Vladivostok* (in Russian).
- Sakhno, V.G., Kovalenko, S.V., Lyzganov, A.V., 2016. Granitoid magmatism of the Arminsky Ore District in the Central Sikhote-Alin, Primorye: U–Pb dating, $^3\text{He}/^4\text{He}$ isotope characteristics, features of petrochemical composition and ore mineralization. *Doklady Earth Sciences* 466 (6), 1–7 (in Russian).
- Şengör, A.M.C., Natal'in, B.A., 1996. Paleotectonics of Asia: fragments of a synthesis. In: Yin, An, Harrison, T.M. (Eds.), *The Tectonic Evolution of Asia*. Cambridge University Press, pp. 486–640.
- Shand, S.J., 1943. *The Eruptive Rocks*. 2nd edn. John Wiley, New York.
- Simanenko, V.P., Khanchuk, A.I., 2003. Cenomanian volcanism of the Eastern Sikhote-Alin volcanic belt: geochemical features. *Geochemistry International* 8, 787–798 (in Russian).
- Simanenko, L.F., Ratkin, V.V., 2008. Partizansky base-metal skarn deposit: geology, mineralogy, genesis: Tauha metallogenic zone, Sikhote-Alin. *Nauka, Moscow* (in Russian).
- Simanenko, V.P., Govorov, I.N., Khetchikov, L.N., Gonevchuk, V.G., Gerasimov, N.S., 1997. The Cretaceous granitoids of Central Sikhote-Alin: intrusive complexes and series, their geodynamic position and origin. *Russian Journal of Pacific Geology* 16 (5), 70–78 (in Russian).
- Simanenko, V.P., Khanchuk, A.I., Golozubov, V.V., 2002. First data on the geochemistry of Albian–Cenomanian volcanism in Southern Primorye, Russia's Far East. *Geochemistry International* 1, 95–99 (in Russian).
- Solovov, S.G., 1995. Geology and genesis of the Skrytoe tungsten deposit in the Central Sikhote-Alin (Russia). *Geology of Ore Deposits* 37 (2), 121–134 (in Russian).
- Utkin, V.P., 1985. Geodynamics of crustal extension in the Asian continent – Pacific Ocean transition zone. *Geotectonics* 1, 73–87 (in Russian).
- Utkin, V.P., 2013. Shear structural paragenesis and its role in continental rifting of the East Asian margin. *Russian Journal of Pacific Geology* 7 (3), 167–188.
- Valui, G.A., Moskalenko, E.Yu., 2010. First data on the isotopes of Sm–Nd and Sr for Cretaceous–Paleogene granitoids of Primor'e and some problems of their genesis. *Doklady Earth Sciences* 435 (1), 1511–1514.
- Valuy, G.A., 2014. Petrology of Granitoids and Differentiation of Melts under Shallow-depth Conditions (East-Sikhote-Alinsky Volcanic Belt). *Dal'nauka, Vladivostok* (in Russian).
- Valuy, G.A., Strizhkova, A.A., 1997. Petrology of Shallow-depth Granitoids on the Example of Dalnegorsk District, Primorye. *Dal'nauka, Vladivostok* (in Russian).
- Whalen, J.B., Currie, K.L., Chappell, B.W., 1987. A-type granites: geochemical characteristics, discriminations and petrogenesis. *Contributions to Mineralogy and Petrology* 95 (4), 407–419.
- White, A.J.R., Clemens, J.D., Holloway, J.R., Silver, L.T., Chappell, B.W., Wall, V.J., 1986. S-type granites and their probable absence in southwestern North America. *Geology* 14 (2), 115–118.
- Wu, F., Sun, D., Li, H., Jahn, B.-M., Wilde, S., 2002. A-type granites in northeastern China: age and geochemical constraints on their petrogenesis. *Chemical Geology* 187, 143–173.
- Zhou, J.-B., Cao, J.-L., Wilde, S.A., Zhao, G.-C., Zhang, J.-J., Wang, B., 2014. Paleo-Pacific subduction-accretion: evidence from geochemical and U–Pb zircon dating of the Nanhada accretionary complex, NE China. *Tectonics* 33, 2444–2466.
- Zimin, S.S., Sakhno, V.G., Govorov, I.N. (Eds.), 1991. *Tectonic Margin of Asia: Magmatism*. Nauka, Moscow (in Russian).